FEBS Letters 412 (1997) 346–350 FEBS 18943

Crystallization, preliminary diffraction and electron paramagnetic resonance studies of a single crystal of cytochrome *P*450nor

Sam-Yong Park[a,*], Hideaki Shimizu[b], Shin-ichi Adachi[a], Yoshitsugu Shiro[a], Tetsutaro Iizuka[a], Atsushi Nakagawa[c], Isao Tanaka[c], Hirofumi Shoun[d], Hiroshi Hori[1,e]

[a]*The Institute of Physical and Chemical Research (RIKEN), Hirosawa 2-1, Wako, Saitama 351-01, Japan*
[b]*Faculty of Science, Gakushuin University, Tokyo 170, Japan*
[c]*Division of Biological Sciences, Graduate School of Science, Hokkaido University, Sapporo 060, Japan*
[d]*Institute of Applied Biochemistry, University of Tsukuba, Tsukuba, Ibaraki 305, Japan*
[e]*Department of Biophysical Engineering, Faculty of Engineering Science, Osaka University, Toyonaka, Osaka 560, Japan*

Received 8 April 1997; revised version received 13 June 1997

Abstract Cytochrome *P*450nor (*P*450nor) is a heme-containing nitric oxide reductase from the denitrifying fungus, *Fusarium oxysporum*. This enzyme catalyzes the reduction of NO to N_2O. In the present study, we report results from preliminary crystallographic and electron paramagnetic resonance (EPR) analysis of a single crystal of *P*450nor. The crystal was grown in 100 mM MES buffer at pH 5.6 using PEG 4000 as a precipitant. It belongs to the orthorhombic system with cell dimensions of $a=54.99$ Å, $b=82.66$ Å, $c=87.21$ Å, and the space group is $P2_12_12_1$. The crystal diffracts synchrotron radiation at higher than 2.0 Å resolution, and therefore it is suitable for X-ray crystal structure analysis at atomic resolution. Bijvoet and dispersive anomalous difference Patterson maps show a clear peak corresponding to the heme iron. The structure solution is currently underway by means of MIR and MAD techniques. EPR analysis determined the orientation of the heme within the *P*450nor crystal.

Key words: Nitric oxide reductase; Cytochrome *P*450; Crystallization; EPR; MAD

1. Introduction

Cytochrome *P*450nor is a heme-containing enzyme which has a molecular weight of 46 000. This enzyme is classified into the *P*450 superfamily on the basis of its amino acid sequence deduced from the DNA analysis [1]. However, the biological function of *P*450nor is very unique, compared with other usual *P*450s. While the usual *P*450s catalyze monooxygenation reaction using O_2, *P*450nor can catalyze the NO reduction but not the monooxygenation [2]. It is reasonable to suggest that some subtle but significant differences in the structure at the active site are responsible for the functional difference between *P*450nor and the usual *P*450s [3–6]. To evaluate such structural differences, we have been making a single crystal of *P*450nor for fine structural analysis by X-ray crystallography. In this paper, we report the crystallization, preliminary crystallographic characterization, and EPR studies of a single crystal of *P*450nor isolated from *Fusarium oxysporum*.

*Corresponding author. Fax: (81) (48) 462-4660.
E-mail: park@postman.riken.go.jp

[1]Corresponding author. Fax: (81) (6) 850-6557.
E-mail: hori@bpe.es.osaka-u.ac.jp

Abbreviations: PEG, polyethylene glycol; MES, 2-(*N*-morpholino)-ethanesulfonic acid; EPR, electron paramagnetic resonance; EDTA, ethylenediaminetetraacetic acid; MIR, multiple isomorphous replacement; MAD, multiwavelength anomalous diffraction

2. Material and methods

2.1. Purification and crystallization

Cytochrome *P*450nor was isolated from the denitrifying cells of *Fusarium oxysporum* according to the procedure of Shoun et al. [7]. The protein was purified using DEAE-cellulose (DE-52, Whatman, UK) and Sephadex G-100 (Pharmacia, Sweden) columns. Protein homogeneity was determined with SDS/PAGE and isoelectronic focusing gel. The sample was stable for several months at 4°C in 20 mM potassium phosphate buffer at pH 7.2 containing 10% (v/v) glycerol, 0.1 mM dithiothreitol and 0.1 mM EDTA. *P*450nor was crystallized with a vapor diffusion using the sitting drop technique. Crystals were grown in 100 mM MES buffer at pH 5.6 using PEG 4000 as a precipitant. The initial drops were composed of the 2 μl protein solution (50 mg ml^{-1}) and of the 2 μl precipitant solution, and were equilibrated with the precipitant solution in a 1 ml reservoir.

2.2. Native diffraction data collection

High-resolution diffraction data were obtained using the synchrotron radiation source at the BL-6A station of the Photon Factory, KEK, Japan. Intensity data were collected with a Weissenberg camera for macromolecular crystallography [8] which was equipped with a 430 mm radius cylindrical cassette. An imaging plate of 400×200 mm^2 was used as a two-dimensional detector. Crystals were mounted with their *a*- or *c*-axis as the axis of rotation. Measurements were carried out at 15°C and wavelength of 1.00 Å to collect native data. Every image data frame was read out on a Fuji Film BA100 imaging plate system (Fuji PhotoFilm Co. Ltd). Data were processed with DENZO [9]. Programs of the CCP4 suite [10] were used for scaling, merging and further calculation.

2.3. Multiwavelength anomalous diffraction (MAD) data collection

Because each protein molecule contains one heme group, we attempted to solve the structure using the multiwavelength anomalous diffraction (MAD) method. All diffraction data sets for MAD calculation were collected from one crystal at beamline 18B of the Photon Factory. Diffraction data sets were recorded on imaging plates [11] mounted on a multifunction camera for macromolecular crystallography [12] with a crystal-detector distance of 430 mm. Three imaging plates were used to collect each frame, and effective detector area was, therefore, 400×600 mm^2. The imaging plates were read with a BAS2000 scanner (Fuji PhotoFilm Co. Ltd). Crystals were mounted so that the *a*-axis was the rotation axis. Measurements were made at 15°C. Prior to diffraction data collection, we measured the fluorescence spectrum of the *P*450nor crystal to determine the absorption edge of the heme iron. On the basis of this data, three different wavelengths (1.735 Å, 1.738 Å, 1.741 Å or 0.900 Å), including absorption edge of iron, were selected for the diffraction data collection. Data was processed as described above.

2.4. EPR measurements

EPR measurements were carried out at X-band (9.23 GHz) micro-

PII S0014-5793(97)00795-3

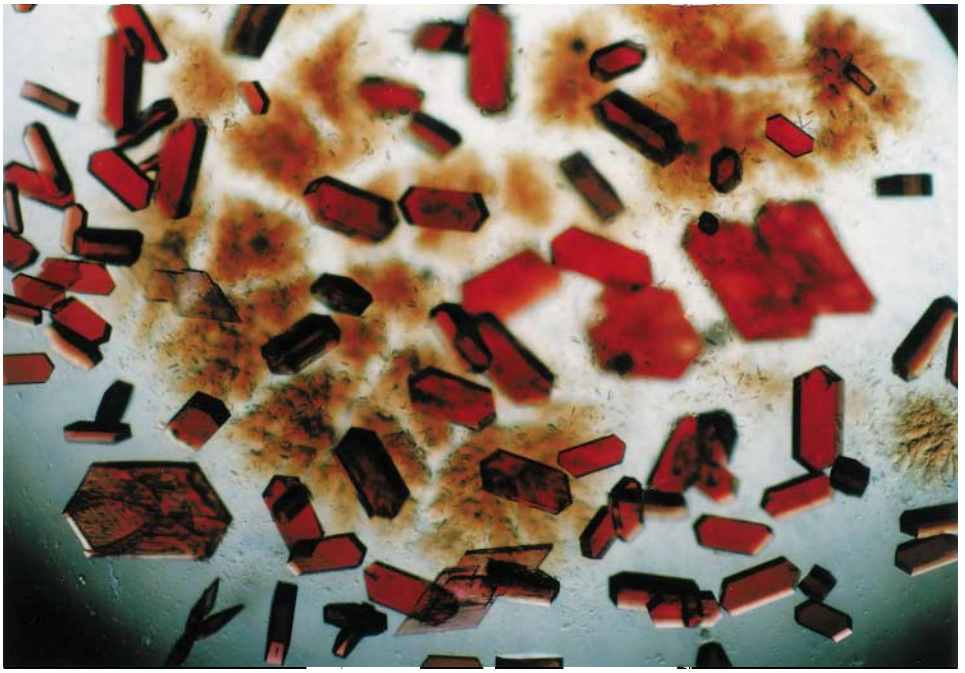

Fig. 1. A single crystal of cytochrome *P*450nor grown from 30% (w/v) PEG 4000, 100 mM MES buffer at pH 5.6. Approximate dimensions of the crystal are $0.7\times0.3\times0.1$ mm^3.

wave frequency with a Varian E-12 EPR spectrometer with 100-kHz field modulation. An Oxford flow cryostat (ESR-900) was used for measurements at 10 K. A custom-built two-circle Teflon goniometer was used for single crystal measurements to rotate sample crystals at 5° or 10° steps with a reproducibility of ± 5°. The principal values and eigenvectors for *g*-tensor, with respect to the crystallographic axes, were determined according to Scholand's method [13].

3. Results and discussion

3.1. Characterization of crystals and analyses of data quality

*P*450nor crystals were obtained within one week at 20°C. Typical size of the crystal we obtained was $0.7\times0.3\times0.2$ mm^3 (Fig. 1). The crystal was orthorhombic space group $P2_12_12_1$, with unit-cell parameters of $a=54.99$ Å, $b=82.66$ Å and $c=87.21$ Å. Assuming that one molecule of *P*450nor protein is contained in an asymmetric unit, crystal volume per protein mass (VM) is calculated as 2.17 Å^3 Da^{-1}. This value corresponds to a solvent content of approximately 41%. This value is within the ranges frequently observed for protein crystals [14]. The reflection data have an *R* merge 5.4% for 24 733 independent reflections derived from 84 152 total observations. The completeness of the data set is 90.1% in the 100–2.0 Å range. The result of data reductions is summarized in Table 1.

Nakahara et al. [15] previously reported a *P*450nor crystal, which had been crystallized in 1.88 M ammonium sulfate (pH 7.2). The crystal belongs to the monoclinic space group $P2_1$, with unit cell dimensions of $a=74.7$ Å, $b=86.7$ Å, $c=62.0$ Å and $\beta=97°$. The crystal gave the diffractions at 2.5 Å resolution limit, but with large mosaicity in the direction perpendic-

Table 1
Result of data reduction of cytochrome *P*450nor

	Native data	MAD data			
Cell constants (Å)	$a=54.99$ $b=82.66$ $c=87.21$	$a=54.97$ $b=80.48$ $c=88.33$			
Wavelength (Å)	1.000	1.735	1.738	1.741	0.900
Resolution (Å)	2.0	2.0	2.0	2.5	2.5
R_{merge}[1]	0.054 (0.107)	0.043 (0.478)	0.038 (0.291)	0.037 (0.306)	0.075
R_{anom}	0.039 (0.116)	0.056 (0.491)	0.046 (0.302)	0.044 (0.344)	0.058
No. of measurements	84 152	36 887	39 526	37 834	47 221
No. of independent reflections	24 733	13 581	13 818	13 624	12 626
Completeness[2]	90.1	50.6	50.6	50.6	91.7
Multiplicity	3.4 (2.1)	2.7 (2.3)	2.9 (2.5)	2.8 (2.4)	3.7 (3.6)
Rejected outliers[3]	936	112	131	108	76
Mean $\langle I/s(I)\rangle$	9.9 (7.0)	15.0 (1.5)	12.6 (2.6)	15.3 (2.4)	9.5 (1.8)

[1] $R_{merge}=\Sigma\Sigma_i|I(h)-I(h)_i|/\Sigma\Sigma_i I(h)$, where $I(h)$ is the mean intensity after rejections.
[2] Most of reflections higher than 3 Å resolution collected at an absorption edge could not be measured because of limitation of the effective area of the detector.
[3] Reflections with intensities differing more than 4.0 $\sigma(I)$ from the weighted mean were rejected.

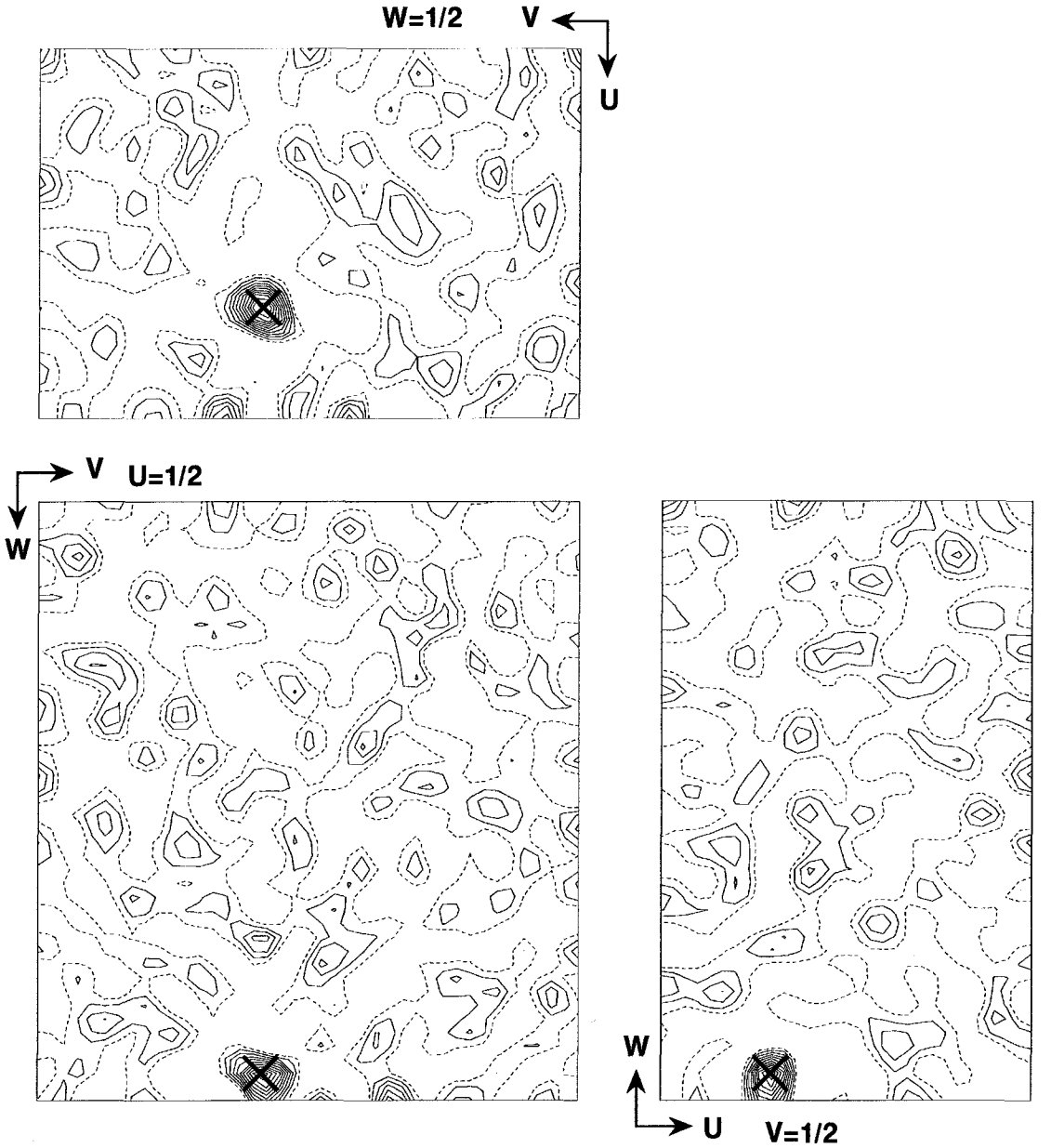

Fig. 2. Bijvoet difference Patterson maps using the data collected at 1.738 Å (PEAK data). Diffraction data between 10 and 3 Å resolution were used for calculation. Cross symbols are corresponding to heme iron-iron self vectors. The position of the heme iron is refined as (0.426, 0.354, 0.760) by the vector-space refinement.

ular to the *b*-axis, suggesting that this type of the crystal was unsuitable for further X-ray crystallographic analyses. In addition, we also obtained a different type of $P2_1$ form of the *P*450nor crystal from the PEG solution (40% PEG 20,000, 100 mM HEPES at pH 7.0) with cell dimensions of $a=55.5$ Å, $b=79.5$ Å, $c=54.0$ Å and $\beta=118°$. This crystal gave X-ray reflections with about 2.5 Å resolution, which were processed in an *R* merge of 10.38% for 34 981 independent reflections derived from 36 050 total observations. However, the crystal is too small ($0.03\times0.03\times0.05$ mm) and cannot be reproducible in another crystallization.

3.2. Position of the heme Fe atom from anomalous dispersion

The crystal for MAD data collection was obtained under the same condition as used for high resolution data collection. One crystal was not isomorphous with other crystals we obtained, and its cell dimensions were shrinked: $a=54.97$ Å, $b=80.48$ Å and $c=88.33$ Å. No serious radiation damage on the crystal was detected during the data collection at four different wavelengths. The result of data reductions is summarized in Table 1. Fig. 2 shows Harker sections of Bijvoet anomalous difference Patterson map using data collected at 1.738 Å. Bijvoet anomalous difference Patterson maps show clear heme iron-iron self vectors on the Harker sections with more than 10 times of r.m.s. deviation of the map. Position of heme iron was refined as (0.426, 0.354, 0.760) by the vector-space refinement [16]. Dispersive anomalous signal was inferior to Bijvoet anomalous difference signal, probably due to scaling error of each data set measured at each wavelength. We tried to solve the structure using MAD data, but anom-

Table 2
The principal g values and the directions in a single crystal at 10 K ($P2_12_12_1$ 4 molecules/unit cell)

P450nor	g-Values	Directional cosine			Angle a,b,c-axes (degree)		
		a	b	c	a	b	c
Low-spin heme 1	$g_x = 1.90$	0.95	0.07	0.30	18	86	72
	$g_y = 2.24$	0.15	−0.96	−0.25	81	−17	−75
	$g_z = 2.50$	0.27	0.29	−0.92	74	73	−23
High-spin heme 1	$g_x = 7.90$	0.96	0.02	0.27	16	89	74
	$g_y = 3.79$	0.08	−0.97	−0.24	85	15	−76
	$g_z = 1.69$	0.26	0.25	−0.93	75	75	−21

alous signals were not large enough for phase determination to obtain an interpretable electron density map.

We also collected three diffraction data sets at three different wavelengths for a crystal which was isomorphous to other native crystals. Anomalous Patterson maps calculated with these data sets showed lower self vector peaks and MAD phasing also failed. However, as this crystal is isomorphous with the other crystals, these data sets may give some phase information during MIR phasing. Preparation of heavy atom derivatives for phase determinations is in progress, and fine structural analysis is going on.

3.3. EPR analysis of a single crystal

The powder EPR spectrum of oxidized *P*450nor at 10 K was characteristic for the ferric low spin species but a small amount of ferric high spin species was also observed as reported previously [17]. The principal g values determined from the powder EPR spectrum ($g_x = 1.91$, $g_y = 2.25$, $g_z = 2.42$ for the low spin species and $g_x = 7.85$, $g_y = 3.40$, $g_z = 1.75$ for the high spin species) were somewhat different from those for the previous results. In order to determine more precise principal g values and eigenvectors, we measured single crystal EPR spectra of the oxidized *P*450nor. From the angular variations of g^2 values for the single crystals, the principal values and eigenvectors of g tensors were determined according to the analytical method of Schonland [13]. The principal values and eigenvectors with respect to the crystallographic axes are listed in Table 2. The four molecules in the unit cell of the $P2_12_12_1$ crystals have g tensors related to each other by 180° rotation about the crystallographic a, b, and c axes. The g values and the direction angles of their principal axes with respect to the crystallographic axes were obtained with a precision of ±0.01 and ±5°, respectively. The principal g values were somewhat different from those estimated from the powder EPR spectrum. These errors were probably derived from the uncertainty of the g values that originated from the line width of the signals and from the uncertainty of mounting the crystals on the sample holder. It should be pointed out that the direction of the maximal g value ($g_{zz} = 2.50$) for the low spin species is very close to the minimal g value ($g_{zz} = 1.69$) for high spin species. From the X-ray crystallographic and EPR studies of aquomet myoglobin, the direction of g_{zz} coincides with the heme normal [18]. Therefore, we assume that the direction of the minimal g value ($g_{zz} = 1.69$) of the high spin species of *P*450nor coincides with the heme normal. The angle between the direction of the g_{zz} of the ferric high spin species and that of the maximal g value (g_{zz}) of the ferric low spin species is 2.8°. If the (x,y,z) axis system is assumed to be fixed in the framework of the heme, the heme plane orientation does not change in passing from the high spin to the low spin species of the oxidized *P*450nor. *P*450nor has predominantly a low spin, and six-coordinated iron with a cystein thiolate and H_2O or OH^- as axial ligands. High spin iron, on the other hand, is typically five-coordinate, in which the sixth liganded water molecule or OH^- is removed. In the present single crystal EPR experiments, we found that the ratio of the contents between the high spin and low spin species was variable from crystal to crystal. This means an occupancy of the water molecule in the distal heme cavity is readily changed during the crystallization. Our recent X-ray crystallographic analyses of *P*450nor indicate that the heme plane orientation in the crystalis coincident with that of the present EPR result.

Acknowledgements: This work was supported in part by the Biodesign Research Program from RIKEN (to T.I. and Y.S.), by the MR Science Research Program in RIKEN (to T.I. and Y.S.), by the SR Structural Biology Program in RIKEN (to Y.S.), by the Sakabe Project at the TARA (Tsukuba Advance Research Alliance) Center, University of Tsukuba, Japan (to H.S.), by the Special Postdoctoral Researchers' Program in RIKEN (to S.-Y.P.) and by a Grant-in-Aid for Scientific Research on Priority Area from the Ministry of Education, Science, Culture, and Sports of Japan (to H.S., H.H. and Y.S.). We thank Prof. N. Sakabe, Dr. N. Watanabe, and Dr. M. Suzuki for their advice in the data collection at PF. Data collection at PF was performed under approval of the PF Program Advisory Committee (Proposal No. 94G253).

References

[1] Kizawa, H., Tomura, D., Oda, M., Fukamizu, A., Hoshino, T., Gotoh, O., Yasui, T. and Shoun, H. (1991) J. Biol. Chem. 266, 10632–10637.
[2] Nakahara, K., Tanimoto, T., Hatano, K., Usuda, K. and Shoun, H. (1993) J. Biol. Chem. 268, 8350–8355.
[3] Poulos, T.L., Finzel, B.C. and Howard, A.J. (1986) Biochemistry 25, 5314–5322.
[4] Ravichandran, K.G., Boddupalli, S.S., Hasemann, C.A., Peterson, J.A. and Deisenhofer, J. (1993) Science 261, 731–736.
[5] Hasemann, C.A., Ravichandran, K.G., Peterson, J.A. and Deisenhofer, J. (1994) J. Mol. Biol. 236, 1169–1185.
[6] Cupp-Vickery, J.R. and Poulos, T.L. (1995) Nature Struct. Biol. 2, 144–152.
[7] Shoun, H., Sudo, Y., Seto, Y. and Beppu, T. (1983) J. Biochem. 94, 1219–1229.
[8] Sakabe, N. (1983) J. Appl. Crystallogr. 16, 542–547.
[9] Otwinowski, Z. (1988) DENZO. A Program for Automatic Evaluation of Film Densities. Yale University, New Haven, CT.
[10] The CCP4 (1994) Acta Crystallogr. D50, 760–763.
[11] Miyahara, J., Takahashi, K., Amemiya, Y., Kamiya, N. and Satow, Y. (1985) Nucl. Instrum. Methods A246, 572–578.
[12] Sakabe, N., Ikemizu, S., Sakabe, K., Higashi, T., Nakagawa, A., Watanabe, N., Adachi, S. and Sasaki, K. (1995) Rev. Sci. Instrum. 66, 1276–1281.
[13] Schonland, D.S. (1959) Proc. Phys. Soc. 73, 788–792.
[14] Matthews, B.W. (1968) J. Mol. Biol. 33, 491–497.

[15] Nakahara, K., Shoun, H., Adachi, S., Iizuka, T. and Shiro, Y. (1994) J. Mol. Biol. 239, 158–159.
[16] Tickle, I.J. (1991) in: Proceedings of the CCP4 Study Weekend (Wolf, W., Evans, P.R. and Leslie, A.G.W., Eds.), pp. 87–95, Science and Engineering Research Council, Daresbury Laboratory, Warrington.
[17] Shiro, Y., Fui, M., Isogai, Y., Adachi, S., Iizuka, T., Obayashi, E., Makino, R., Nakahara, K. and Shoun, H. (1995) Biochemistry 34, 9052–9058.
[18] Bennet, J.E., Gibson, J.F. and Ingram, D.J.E. (1957) Proc. R. Soc. Lond. A 240, 67–82.